Acta Cryst. (1968). A24, 206

A Wave Mechanical Description of Electron and Positron Emission from Crystals

BY R.E. DEWAMES AND W.F. HALL
North American Aviation Science Center, Thousand Oaks, California, U.S.A.

(*Received* 7 *June* 1967 *and in revised form* 12 *September* 1967)

A wave mechanical treatment of the spatial dependence of the intensity for positrons and electrons emitted from a radioactive source embedded in a crystal is developed. The predicted intensity pattern is found to be characterized by Bragg angles and Bragg widths and as such cannot be derived from a classical treatment.

1. Introduction

Recently Uggerhøj (1966) measured the orientation dependence of the intensity of β^+ and β^- particles emitted from ^{64}Cu embedded in a copper lattice [Fig. 1(*a*)]. Because of the remarkable similarity between the emitted intensity observed for the positron and that observed for heavier charged particles under the same conditions of emission [see Fig. 1(*b*); Domeij (1966)] Uggerhøj compared his measured angular widths with the predictions of the classical mechanical theory developed by Lindhard (1965) for the motion of charged particles in a crystal lattice. As he obtained substantial agreement with Lindhard's critical angle ψ_1, he concluded that his measured intensities were just another manifestation of classical channeling and blocking phenomena.

It is well known that the phenomena observed in the electron microscope must be described in terms of wave interference; Bragg angles and resonance widths dominate the intensity patterns even when the electron wavelength is very much smaller than the lattice spacing of the target crystal. Yet, wave interference has been dismissed in the description of channeling experiments such as those of Uggerhøj on the basis that the DeBroglie wavelength is small.

No one can doubt that there is, indeed, a limit in which classical mechanics can be used to describe the motion of particles in crystals. But, in view of the discrepancy mentioned above, it becomes necessary to ask under what conditions the correspondence limit is obtained. The classical picture of the emission of a particle from a lattice site in a crystal envisions the particle leaving its parent atom with a definite, but random, momentum; those particles which leave at large angles to the crystal planes encounter an essentially amorphous environment and contribute a uniform background of intensity outside the crystal; those particles which leave at a small angle to a crystal plane are heavily influenced by the average potential in that plane, so that positively charged particles are driven away from their initial directions, giving a minimum of intensity parallel to the plane, while negatively charged particles may become trapped by the planar potential, tending to emerge from the crystal parallel to the trapping plane.

The quantum mechanical solution of the emission problem yields a spherical wave for the initial amplitude of the emitted particle, with equal amplitude in all directions. Because of the phase coherence of this emitted wave, the scattering of the wave from the periodic array of crystal atoms introduces marked interference effects in the emitted intensity. This is in contrast to the classical view of the initial conditions, a view which corresponds quantum mechanically to starting a particle as a wave packet localized to within a small fraction of a lattice spacing of the emitter, with some large momentum, defined to within the limits set by the uncertainty principle. This version of the initial conditions obviously restricts interference effects to a minimum, since they can only arise owing to the spread of the wave packet as it moves through the crystal.

The problem of the intensity pattern outside a crystal due to a source inside the crystal was solved by von Laue in the 1930's, in order to explain the bands observed by Kikuchi when electrons scattered inelastically inside the crystal. Both the theoretical development and many examples of the observed patterns can be found in his book, *Materiewellen und Ihre Interferenzen*, published in 1948.

Basically, one must consider the propagation of the original spherical wave as a superposition of Bloch waves inside the crystal, taking appropriate boundary conditions at the crystal surface to determine the intensity pattern outside. To describe accurately the resulting intensity, several Bloch waves are needed, which greatly complicates the analytical task. However, the most important features of the emission can be recovered from a consideration of only one or two Bragg reflections. The analysis in terms of these simpler problems is discussed in § 3. In later sections, contact is made with the experimental observations of Uggerhøj and consequences leading to possible further experiments are discussed.

2. Theoretical development

The emission of a particle from a point r' inside a crystal can be described by the following approximation to the many-particle Schrödinger equation (Laue, 1948):

$$\left[\frac{-\hbar^2\nabla^2}{2m}+U(r)-E\right]\varphi(r)=\delta(r-r')\,, \qquad (1)$$

where $\varphi(r)$ is the probability amplitude for the particle propagating without loss of energy, $U(r)$ is an effective periodic potential which is primarily determined by the potential of interaction between a single lattice atom and the emitted particle, E is the energy of the emitted particle, and m is its mass. Inelastic (energy loss) scattering of the emitted particle introduces an imaginary part of $U(r)$ whose form is determined by the cross-section for inelastic scattering in the crystal.

To calculate the intensity pattern of the emission outside the crystal, it is convenient to use the reciprocity relation introduced by von Laue, which gives the intensity at a point r_A outside the crystal due to a point source inside in terms of the intensity at that source point r_B due to a spherical wave emitted from

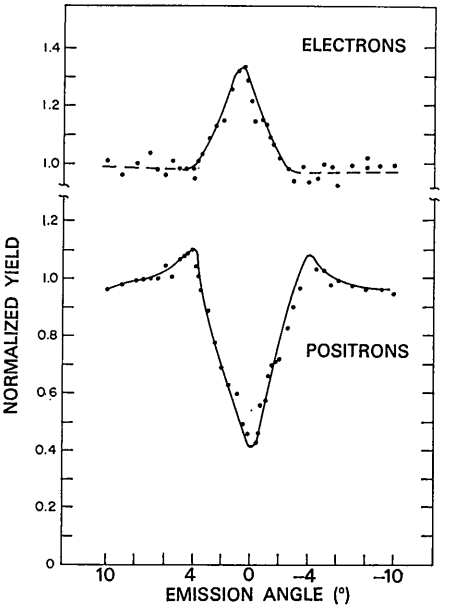

(*a*)

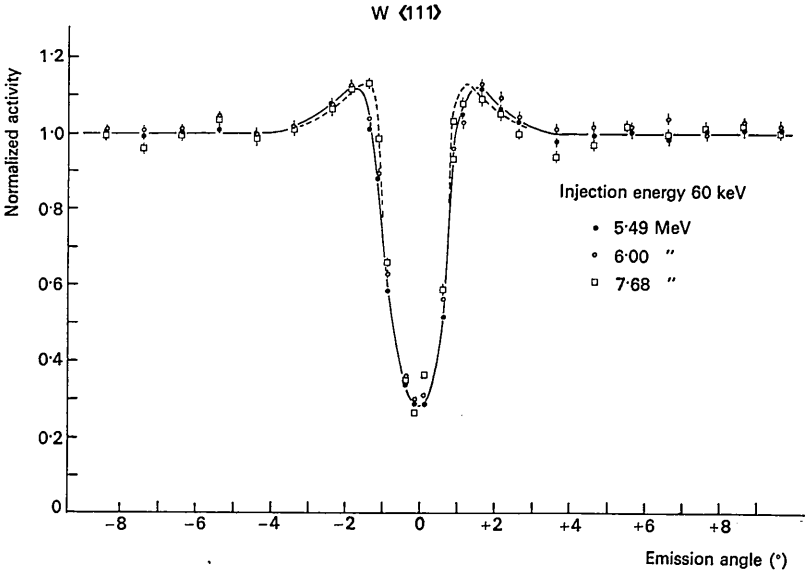

(*b*)

Fig. 1. (*a*) Emission yield of positrons and electrons from copper *versus* angle between emission direction and the [100] axis. The energy of positrons and electrons is 200–300 keV and 150–300 keV, respectively (Uggerhøj, 1966). (*b*) The intensity distribution of the three α-particle groups as a function of polar angles illustrating directional effects (Domeij, 1966).

the point of observation:

$$\varphi(r_A)=\bar{\varphi}(r_B)\,,$$

where $\bar{\varphi}(r_B)$ (the reciprocal wave) is the solution to equation (1) with the source point r' outside the crystal, at r_A.

When the observation is made sufficiently far from the crystal, the spherical wave emitted at r_A reaches the crystal essentially as a plane wave. This allows one to obtain the amplitude inside the crystal by matching the Bloch wave eigenfunction for a particle inside the crystal to the incoming plane wave at the entrance surface. The solution to this problem is discussed, for example, in an earlier paper by DeWames, Hall & Lehman (1966) (henceforth referred to as I). Essentially, the problem is reduced to solving equation (1) for an infinite crystal, without the source term. Expanding the periodic potential $U(r)$ and the amplitude $\varphi(r)$ in Bloch wave form, one has

$$(2\delta_0+\zeta_h)u_h+\sum_g \psi_{h-g}u_g=0\,, \qquad (2)$$

where we have written

$$\varphi(r)=\exp(i\mathbf{k}_M\,.\,\mathbf{r})\sum_h u_h(k_M)\exp i\mathbf{k}_h\mathbf{r})$$

$$\frac{U(r)}{E}=\sum_h \psi_h \exp(i\mathbf{k}_h\,.\,\mathbf{r})$$

$$\frac{\hbar^2}{2m}k_M^2-E=2\delta_0 E\,,\frac{\hbar^2}{2m}[k_h^2+2\mathbf{k}_h\,.\,\mathbf{k}_M]=\zeta_h E\,. \quad (3)$$

The sums in equations (2) and (3) run over all reciprocal lattice vectors $\mathbf{k}_h$. However, as was shown in I, for electrons and positrons at energies larger than a kilovolt, one need only consider a few terms in these sums.

If one restricts the sums in equations (2) and (3) to N terms, there will be N independent solutions for δ_0, and hence for the Bloch wave coefficients u_h, all belonging to the same energy E. These solutions must be superposed to obtain a wave function which matches properly onto the plane wave which is incident on the surface of the crystal from the direction of the point of observation. Neglecting the reflected wave, one can write the boundary conditions as

$$\varphi=\sum_j A_j \exp(i\mathbf{k}_M^{(j)}\,.\,\mathbf{r})\sum_h u_h^{(j)}\exp(i\mathbf{k}_h\,.\,\mathbf{r})$$
$$=\exp(i\mathbf{k}_0\,.\,\mathbf{r}) \quad (4)$$

for all $\mathbf{r}$ such that $\hat{\mathbf{n}}\,.\,\mathbf{r}=0$
where $\hbar^2k_0^2/2m=E$, $\hat{\mathbf{n}}$ is the direction of the inward normal to the crystal surface, and the superscript j is used to label the roots of equation (2).

One satisfies these boundary conditions by choosing (Zachariasen, 1946)

$$\mathbf{k}_M^{(j)}=k_0+k_0^2\delta_0^{(j)}\hat{n}/\mathbf{k}_0\,.\,\hat{n}\,, \qquad (5)$$

and calculating the coefficients A_j from equation (4). Note that in order that equation (5) be consistent with the previous definition of δ_0 in equation (3), $\delta_0 \ll 1$.

Finally, one employs the reciprocity relation to determine the intensity observed outside the crystal by evaluating φ at the point where the particle was emitted.

3. Qualitative features of the intensity

The intensity pattern which one observes outside a crystal for a source placed inside exhibits considerable structure, as will become apparent from the results to

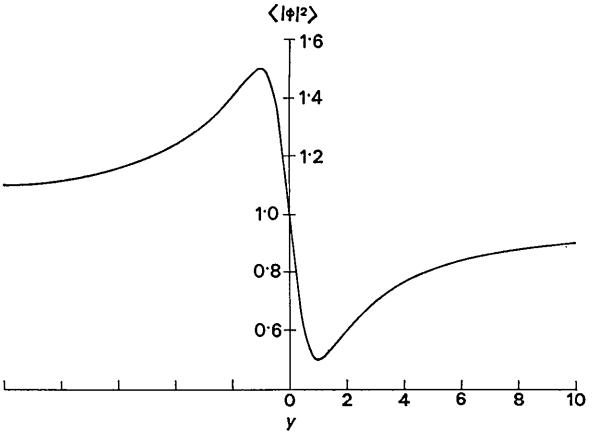

Fig. 2. Angular intensity variation about the Bragg angle, no attenuation.

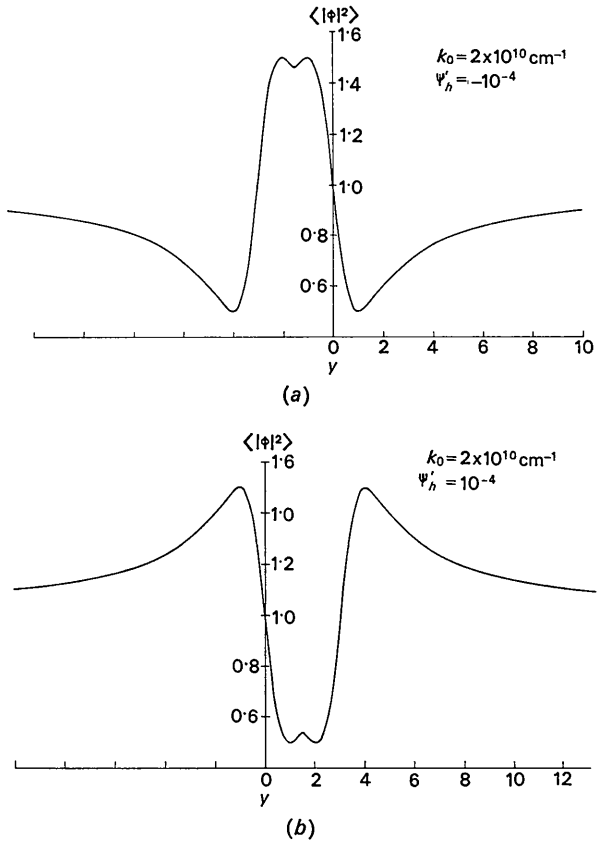

Fig. 3. Angular intensity variation for (*a*) the electron and (*b*) the positron. Two-wave solution, no attenuation.

be presented later on. However, almost all the features which appear can be understood in terms of the behavior of the intensity which one obtains for the case of a single Bragg reflection.

Specializing to the case of an emitter located at a lattice site,* one finds that the two-wave (one Bragg reflection) solution takes the form

$$|\varphi(t)|^2 = x^2 \exp\left[-\left\{1-\frac{\varepsilon_h}{\sqrt{1+y^2}}\right\} t/\xi_0''\right] + (1-x)^2 \exp\left[-\left\{1+\frac{\varepsilon_h}{\sqrt{1+y^2}}\right\} t/\xi_0''\right] + 2x(1-x)\exp\{-t/\xi_0''\}\cos\{\sqrt{1+y^2}\; t/\xi_h'\} \quad (6)$$

where

$$x=\tfrac{1}{2}\left\{1+\frac{y-1}{\sqrt{1+y^2}}\right\}$$

* If the emitter is located in an interstitial site such as midway between two atomic sites, then intensity maximum becomes minimum and *vice versa*, provided that the $\xi_h'' \gg t$.

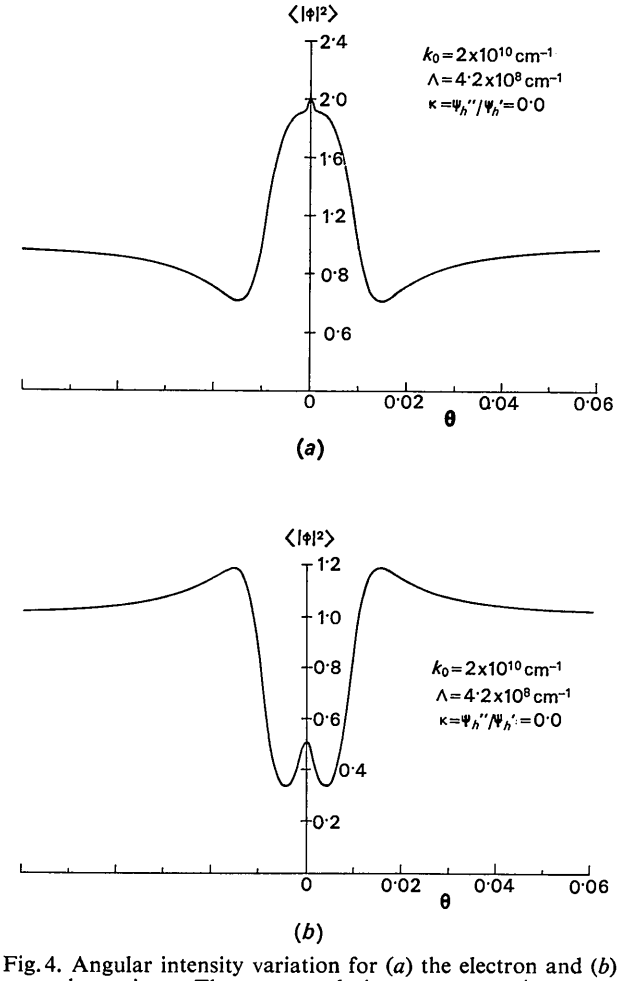

Fig. 4. Angular intensity variation for (*a*) the electron and (*b*) the positron. Three-wave solution, no attenuation.

$$\begin{aligned} y &= \zeta_h/2\psi_h' \qquad (\mathrm{Re}\;\psi_h=\psi_h') \\ \varepsilon_h &= \psi_h''/\psi_0'' \qquad (\mathrm{Im}\;\psi_h=\psi_h'') \\ \xi_h' &= (k_0\psi_h')^{-1}, \quad \xi_h'' = -(k_0\,\mathrm{Im}\;\psi_h)^{-1} \end{aligned} \quad (7)$$

and t is the distance of the emitting atom from the crystal surface. Here we have assumed the imaginary part of the lattice potential U to be small compared with its real part, which is justified for electrons and positrons in the keV range and above (I). In what follows, we have taken the basic interaction potential between the lattice atom and the emitted particle to be a screened Coulomb,* calculating ψ_h' and ψ_h'' as discussed in I. For all the calculations in the present paper, we have used the copper lattice at 0°K as our model crystal.

The extinction distance ξ_h' is typically less than 100 Å for electron energies above 100 kV, while the absorption length ξ_0'' is about 10 times ξ_h'. Thus, a collection of emitting atoms spread over several extinction distances from the crystal surfaces, such as might be achieved by bombarding the crystal with radioactive atoms at a definite energy, will give an intensity which is the average of equation (6) over the thickness. This average will eliminate the cosine term, leaving only the exponentials, with the average distance to the emitter replacing t.

In Fig. 2 we have sketched the thickness averaged intensity one obtains for the two-wave case as a function of angle measured from the Bragg condition when the absorption length is taken to be infinite (no attenuation). The scale y is approximately given by

$$y \simeq \frac{\sin 2\theta_B}{\psi_h}(\theta_B-\theta) \quad (8)$$

so that its value at $\theta=0$ (looking straight down the planes) depends on the magnitudes of ψ_h' and the Bragg angle.

Fig. 3 shows the intensity pattern one might expect from including the Bragg reflection on the other side of $\theta=0$. It is constructed by reflecting the curve of Fig. 2 about $\theta=0$, which for the positron occurs at $y=+1{\cdot}5$, and for the electron at $y=-1{\cdot}5$, for the conditions shown in the Figure.

In Fig. 4 we have sketched the true three-wave solution for the intensity, for the same conditions as in Fig. 2. The dip for the positron and the enhancement for the electron are correctly predicted from the two-wave solution. However, the wings on these two curves are significantly reduced in size. Also, the electron fails to show any cusp at $\theta=0$, whereas the positron shows a marked rise at the origin.

When attenuation is added to the problem, the enhancement above background disappears and the intensity minimum shifts toward the Bragg angle. The two-wave prediction for the intensity about $\theta=0$ compares quite well with the three-wave solution, which is displayed in Fig. 5. The only significant change in

* $U(r)=(1+i\kappa)Ze^2\exp(-\Lambda r)/r$.

going to the three-wave case is a lowering of the value at $\theta=0$ relative to background.

It is interesting to note the similarity in shape and relative magnitude between the positron intensity pattern observed by Uggerhøj (Fig. 1) and the curve of Fig. 4(*b*). There is, however, one significant difference: the wings in Fig. 4(*b*) occur at about $2\theta_B$, whereas for the energies used by Uggerhøj, the wings occur at about $8\theta_B$. In the next section we shall see how this discrepancy might be explained.

4. Relation to experiment

The intensity emitted in an arbitrary direction from the crystal in general is influenced by many simultaneous Bragg reflections due to different sets of intersecting planes. For instance, Uggerhøj observed the intensity in the neighborhood of the copper [001] direction, where four different sets of planes intersect. The geometry for his experiment is represented schematically in Fig. 6, with lines drawn at $2\theta_B$ to indicate the position of the 'wings' about each plane.

The smallest number of waves one can hope to use in describing such a situation is *nine*, which makes the interpretation of the measured intensity somewhat difficult. However, one can say that structure is expected to show up in the intensity pattern at angles which intersect any of the 'wings'.

A computer calculation for the geometry of Fig. 6 for no attenuation gives the results shown in Figs. 7 and 8. Neglecting attenuation is appropriate for the experiment of Uggerhøj because the β mean free path at his energies is long compared with the mean depth of the emitters. Fig. 7 shows the intensity which would be observed moving exactly parallel to the (020) plane. The most important feature to notice here is that the intensity does not return to background for large θ. This is because one remains at $\theta=0$ relative to the plane one is travelling along, and in the absence of the other planes there would be essentially no variation along the band.

In Fig. 8 the path of observation makes an angle of $11\frac{1}{4}°$ with the (020) plane, as illustrated by the line labelled 2 in Fig. 6. Here one notices that the final 'wing' is crossed at an angle of about 4° ($8\theta_B$). Also, at large θ one slowly returns to background ($|\varphi|^2=1$). The structure one encounters prior to the final 'wing' is negligible for the positron, constituting an essentially broad minimum in the intensity. For the electron, the structure for $\theta<8\theta_B$ is much more pronounced, with a relatively sharp peak at $\theta=0$, followed by a shoulder and a second maximum where the 'wing' for the (200) and (220) planes are intersected.

At this stage, one can only suggest that these were the conditions under which Uggerhøj made his measurements. Certainly, the similarity in structure, both for the positron and the electron, is striking.

Clearly, it is worthwhile to try to simplify the experimental situation and to consider other types of experiments which can distinguish between the classical interpretation of electron motion in terms of channeling and blocking, and the wave mechanical interpretation in terms of Kikuchi bands. The most obvious experiment of this type is to measure the separation of the 'wings' of the intensity pattern in a region where only one plane contributes to the intensity, *e.g.* far out from the symmetry direction. This separation should reduce to $2\theta_B$. With regard to attenuation, it must be pointed out that the intensity we have calculated, *e.g.*

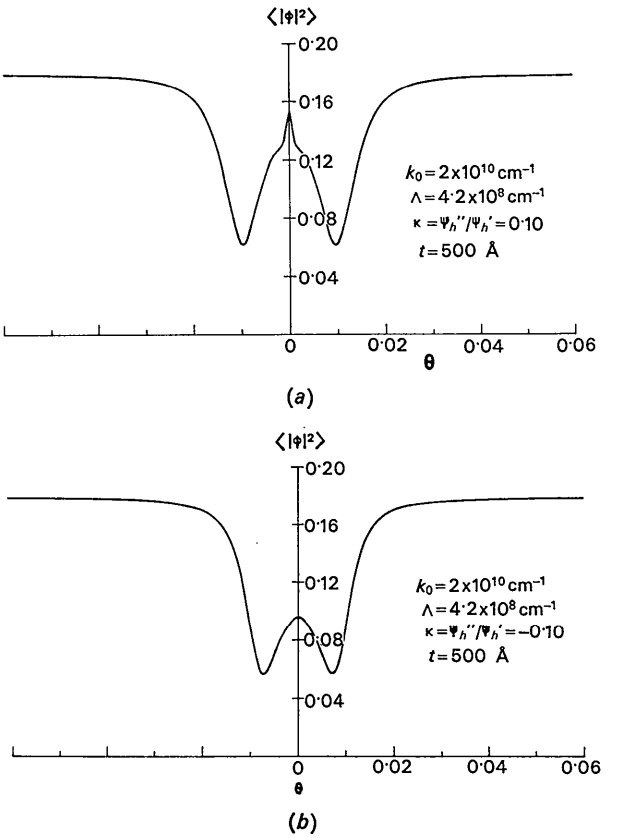

Fig. 5. Angular intensity variation for (*a*) the electron and (*b*) the positron. Three-wave solution with attenuation.

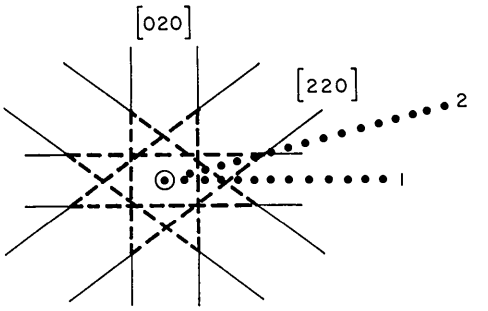

Fig. 6. Geometry in the neighborhood of the [001] axis. The solid lines are drawn approximately at $2\theta_B$ about each plane. The dotted lines 1 and 2 are directions along which intensity variations are plotted in Figs. 7 and 8, respectively.

in Fig. 5, applies only to the beam which has lost no energy. Thus, to make a meaningful comparison when the depth of the emitter is greater than the absorption length, it is necessary to select out the particles which have their original energy. This requires a mono-energetic source, which can be achieved for electrons by utilizing the K-conversion electrons resulting from a sharp nuclear transition.

5. Contribution of additional Bragg reflections

The analysis and discussions above were all based on an essentially three-wave description of the intensity pattern arising from a single plane. When higher order reflections for the same plane are included, one obtains the sharp structure shown in Fig. 9. However, the envelope of the intensity in Fig. 9 is still well represented by the three-wave solution. Essentially, one has superimposed on this envelope the two-wave solution for the higher order reflections (compare Fig. 2); the widths are relatively sharper owing to the decrease of ψ_h and the increase of θ_B with increasing order [see equation (8)].

6. Concluding remarks

In the preceding sections we have shown that the experimental results of Uggerhøj can be interpreted in terms of a wave mechanical description of the scattering of the emitted particles. This description yields a structure for the emitted intensity whose characteristic angles are the Bragg angle and the width of the Bragg resonance [equation (8)]. Therefore, in this limit the results of the dynamical theory are incompatible with the classical mechanical treatment.

One may well ask under what conditions it is valid to use a classical description of particle motion in crystals. To this end, we have recently expanded our investigations to include more massive particles, such as the proton and neutron, and a variety of potentials of interaction.

What we find is that the intensity approaches a limiting form independent of $\hbar$ when the interaction potential is sufficiently strong or the mass is sufficiently large.

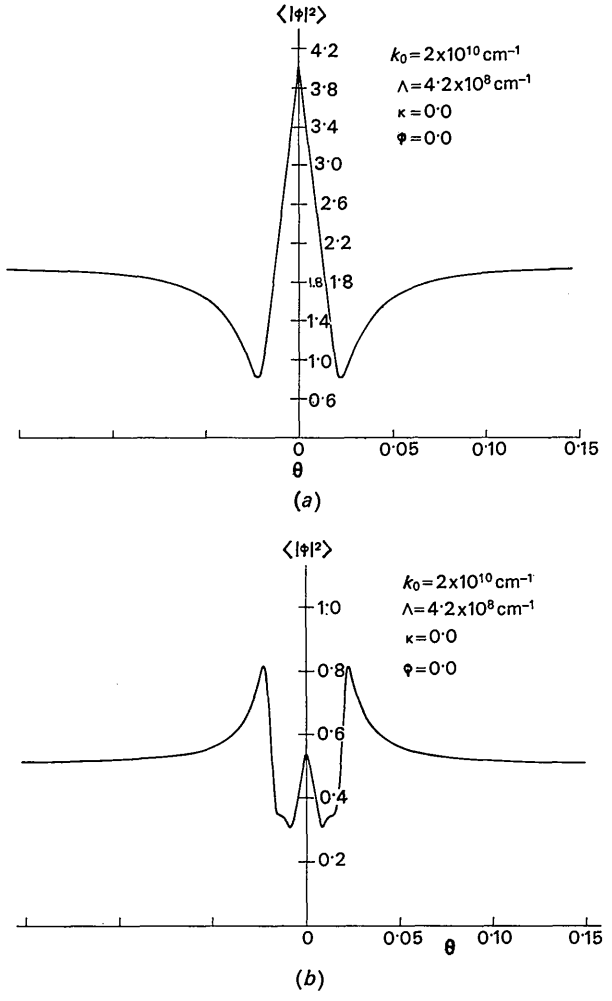

Fig. 7. Angular intensity variations for (*a*) the electron and (*b*) the positron along line 1, Fig. 6. Nine-wave solution, no attenuation.

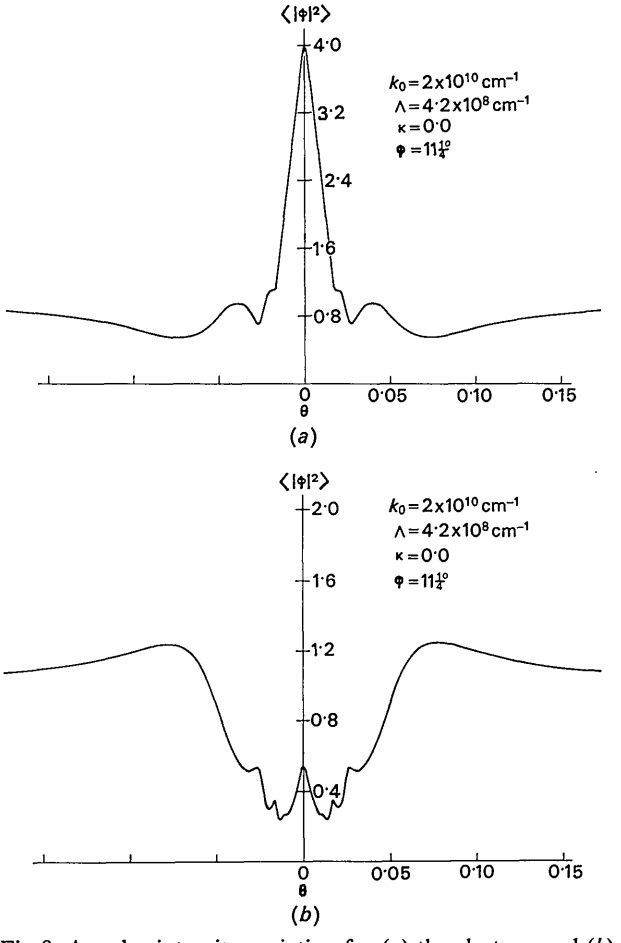

Fig. 8. Angular intensity variation for (*a*) the electron and (*b*) the positron along line 2, Fig. 6. Nine-wave solution, no attenuation.

The criterion for the applicability of this limit is that the width of the Bragg resonance be large compared with the Bragg angle:

$$\left| \frac{2V_h}{\hbar^2 k_h^2/2m} \right| = \frac{\Delta\theta_B}{\theta_B} \gg 1 .$$

For neutrons, $\Delta\theta_B/\theta_B$ is actually very small; consequently the angular structure is controlled by Bragg angles. For protons and α particles, on the other hand, $\Delta\theta_B/\theta_B$ is of the order of 10^3, so that the limiting form is very closely approached. This form agrees quite well with the observed α-particle emission patterns and appears to be the proper classical limit for this problem.

In order to carry out the above investigations within the framework of the dynamical theory, it was necessary to employ computer solution of the basic matrix equations [*cf.* equations (2) and (3)]. However, our results strongly suggest that one should be able to treat the approach to the classical limit of particle motion in crystals within a relatively simple analytical framework. We are currently working to develop such a treatment, which then can be directly applied to the design and interpretation of experiments made with the heavier mass charged particles.

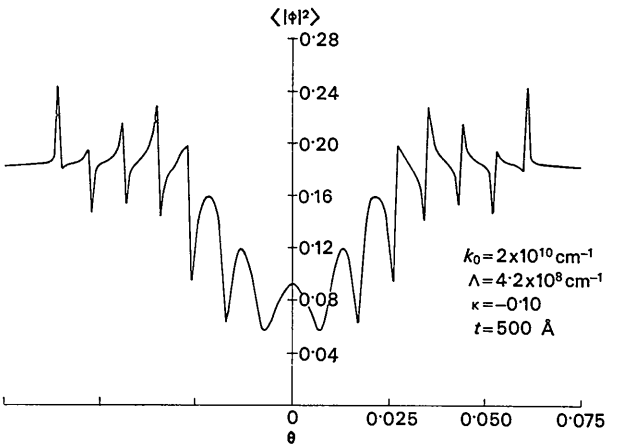

Fig. 9. Angular intensity variation for the positron. Ten-wave solution with attenuation.

References

UGGERHØJ, E. (1966). *Physics Letters*, **22**, 382.

DOMEIJ, B. (1966). *Ark. Fys.* **32**, 179.

LINDHARD, J. (1965). *Mat. Fys. Medel, Dan. Vid. Selsk.* **34**, no. 14.

LAUE, M. VON (1948). *Materiewellen und ihre Inteferenzen.* Leipzig: Akademische Verlagsgesellschaft, Geest & Portig, A. G.

DEWAMES, R. E., HALL, W. F. & LEHMAN, G. W. (1966). *Phys. Rev.* **148**, 181.

ZACHARIASEN, W. H. (1946). *Theory of X-Ray Diffraction in Crystals.* New York: John Wiley. London: Chapman & Hall.

Acta Cryst. (1968). A**24**, 212

Experimental Tests of the General Formula for the Integrated Intensity of a Real Crystal

BY W. H. ZACHARIASEN

Department of Physics, University of Chicago, Chicago, Illinois, U.S.A.

(*Received* 3 *May* 1967)

The new formula for the integrated intensity of a real crystal has been tested experimentally with small crystal spheres of hambergite and of α quartz, and Mo $K\alpha$ as well as Cu $K\alpha$ radiation. Although both materials show very large extinction effects, excellent agreement is obtained between theory and experiment. Discrepancies between predicted and observed integrated intensities seem to be due to inadequately known atomic scattering powers and to experimental errors rather than to a failure of the theoretical formula. The mean radius of the perfect crystal domain was found to be $1{\cdot}98\times10^{-4}$ cm for the hambergite sphere and $0{\cdot}47\times10^{-4}$ cm for the quartz sphere.

Introduction

A new general formula for the integrated intensity, $\mathscr{P}$, of a real crystal was recently reported (Zachariasen, 1967*a*,*b*). It was hoped that this new intensity expression would be valid over the entire range from the ideally imperfect to the perfect crystal, and thus provide for significant improvement in the accuracy of experimental determinations of electron distributions, atomic scattering powers, and of the positional and thermal parameters of the structure. However, in order to obtain even approximate solutions of the basic equations it was necessary to introduce a number of simplifications in the course of the derivation of the intensity formula. It is accordingly highly desirable to explore the validity of the approximations by comparisons with experiment for an assortment of crystal specimens. This paper gives the results of such tests for two crystals with large extinction effects, namely hambergite (Be_2BO_3OH) and α quartz.